

Article

A Study on the Removal of Copper (II) from Aqueous Solution Using Lime Sand Bricks

Xiaoran Zhang ^{1,3,4}, Shimin Guo ¹, Junfeng Liu ^{2,*}, Ziyang Zhang ^{1,3,4} , Kaihong Song ¹,
Chaohong Tan ^{1,3} and Haiyan Li ^{1,3,4,*}

¹ Key Laboratory of Urban Stormwater System and Water Environment, Ministry of Education, Beijing University of Civil Engineering and Architecture, Beijing 102616, China; zhangxiaoran@bucea.edu.cn (X.Z.); gsm0817@163.com (S.G.); ziyangzhang@126.com (Z.Z.); skh201311@163.com (K.S.); chaohongtan@126.com (C.T.)

² Department of Water Conservancy and Civil Engineering, Beijing Vocational College of Agriculture, Beijing 102442, China

³ Beijing Engineering Research Center of Sustainable Urban Sewage System Construction and Risk Control, Beijing University of Civil Engineering and Architecture, Beijing 100044, China

⁴ Beijing Advanced Innovation Center for Future Urban Design, Beijing 100044, China

* Correspondence: liujunfeng@bvca.edu.cn (J.L.); lihaiyan@bucea.edu.cn (H.L.); Tel.: +86-10-6120-9290 (H.L.)

Received: 30 December 2018; Accepted: 8 February 2019; Published: 15 February 2019



Featured Application: This article provides basic knowledge and guidance for the application of construction waste bricks as filling materials in the infiltration facilities such as permeable pavements for the removal of heavy metals.

Abstract: Heavy metals such as Cu(II), if ubiquitous in the runoff, can have adverse effects on the environment and human health. Lime sand bricks, as low-cost adsorbents to be potentially applied in stormwater infiltration facilities, were systematically investigated for Cu(II) removal from water using batch and column experiments. In the batch experiment, the adsorption of Cu(II) to bricks reach an equilibrium within 7 h and the kinetic data fits well with the pseudo-second-order model. The sorption isotherm can be described by both the Freundlich and Langmuir model and the maximum adsorption capacity of the bricks is 7 ± 1 mg/g. In the column experiment, the best removal efficiency for Cu(II) was observed at a filler thickness of 20 cm, service time of 12 min with a Cu(II) concentration of 0.5 mg/L. The Cu(II) removal rate increases with the increasing bed depth and residence time. The inlet concentration and residence time had significant effects on the Cu(II) removal analyzed by the Box–Behnken design (BBD). The Adams-Bohart model was in good agreement with the experimental data in representing the breakthrough curve. Copper fractions in the bricks descend in the order of organic matter fraction > Fe-Mn oxides fraction > carbonates fraction > residual fraction > exchangeable fraction, indicating that the lime sand bricks after copper adsorption reduce the long-term ecotoxicity and bioavailability to the environment.

Keywords: lime sand bricks; copper; batch adsorption; column; sequential extraction

1. Introduction

With the rapid development of urbanization, the increase of impervious areas has interrupted the water infiltration channel, which has greatly increased the rainfall runoff and peak discharge [1]. The heavy metals in urban stormwater runoff mainly come from automobile exhaust, industrial smoke and fossil fuel combustion, dust and various metal facilities. Heavy metals such as copper, zinc and lead are common components in stormwater runoff and usually with relatively high concentrations. Unlike organic pollutants, heavy metals are difficult to degrade in the environment and are easily

accumulated in the human body through the food chain. Excessive intake of heavy metals in the human body may irritate the mucous membranes, leading to liver and kidney damage, capillary damage and central nervous system problems [2]. Cu(II) is essential for some biosyntheses in the human body, and micronutrients as animals and plants are well known, but it is toxic with high concentrations. When the concentration is above the threshold level, it can cause anemia and gastrointestinal discomfort. Infiltration facilities such as permeable pavements could remove pollutants in urban runoff to some extent. Typical pavement systems are mainly composed of materials such as sand and gravel. Because of the unique properties of these media, the adsorption capacity is very limited. The removal of heavy metals in runoff is mainly through the interception of pores in the media. However, with the operation of the permeable paving system, the problem of pore blockage, which is the bottleneck of the operation of the currently trapped system, also results in a significant reduction in the continuous retention of contaminants. In addition, with the long-term operation of the system, the extremely limited adsorption capacity was not able to achieve good removal efficiency for pollutants. Therefore, improving the adsorption capacity of the pavement system medium towards pollutants has a positive effect on reducing the water quality risks.

In many countries, construction and demolition wastes are the main types of wastes in terms of weight. In Europe, more than 30% (*w/w*) of wastes generated is waste bricks. The production of brick-concrete construction wastes in China has been currently increasing year by year. The amount of this type of wastes accounts for 30% to 40% of the total amount of municipal waste. A large amount of construction wastes has piled up, which seriously pollutes the city's atmosphere, water and soil environment, and has a local impact on people's production and life. Recently, there has been an increasing interest in using construction wastes as adsorbents to remove pollutants from wastewater or stormwater. Construction waste bricks are used as the packaging media in percolation facilities. Using construction wastes in remediation were proposed as an alternative method to replace the current methods with a relatively high cost [3]. Due to many economic advantages, construction waste bricks are cheaper than other alternative adsorbents, such as activated carbon, natural and synthetic zeolites, and ion exchange resins. Wilson et al. showed that concrete blocks, crushed stone beds, and geotextiles in the permeable paving system can retain hydrocarbon contaminants and improve the quality of effluent [4]. Wang et al. confirmed that using construction wastes as bioretention media can remove 90% of heavy metals in rainwater [1]. Hussain et al. showed that brick kiln chimney wastes could efficiently remove chromium from solutions and the removal capacity could reach 38.8 mg/g [5].

Although the results of using construction waste bricks to remove heavy metals are promising, there is still a need to better understand the removal efficiency and operational process such as how inlet concentration and residence time affect the removing of pollutants. Nnadi et al. confirmed that a permeable paving system with plastic or stone can effectively remove heavy metals and the mechanism may be chemical sedimentation [6]. Katherine et al. used limestone or zeolite to remove heavy metals from constructed wetlands with a removal efficiency of 98% [7]. Some studies have shown that construction bricks have a good anchoring effect on heavy metals [8], but the research is blurry with regards to the chemical form and content of heavy metals in the media, and the stability after fixing is worth exploring. There are also some studies to remove heavy metals from water using hazelnut and almond shells [9], but these adsorbents are present in small quantities. In addition, there is little research on the existing form of heavy metals after being fixed by the percolation facility and after the environmental risk has been evaluated. Some studies have shown that the shape of the breakthrough curve is affected by the linear velocity, the concentration of metal ions in the solution, and the height of the bed [10–14]. A study found that continuous column experiments can provide good references for environmental remediation applications such as infiltration facilities like permeable pavements [15]. Various models such as the Adams-Bohart model and the Thomas model have been applied to analyze and interpret the experimental data and predict the effects of different process variables on the efficiency of the adsorption process [16]. Chu et al. found that the Adams-Bohart model is essentially the same as the Thomas model [17]. However, heavy metal removal by wastes

bricks should be explored and the proper fitting models should be evaluated in order to better predict the removal behavior.

In the present study, the cost-effective lime sand bricks were selected as the adsorbent, their removal efficiency towards Cu(II) in aqueous solution was systematically studied through the static batch experiments and fixed bed continuous column experiments. The objectives of this study are (i) to study the adsorption mechanism of Cu(II) by lime sand bricks using batch experiments; (ii) to examine the effects of several process parameters such as the bed depth, solution concentration and residence time on removal efficiency of Cu(II); (iii) to analyze the effect of different process variables on the removal of Cu(II) by lime sand bricks and their applicability with the fitting model; (iv) to analyze the chemical forms of copper in the medium of lime sand bricks for the evaluation of the environmental risk.

2. Materials and Methods

2.1. Materials

Lime sand bricks were grounded before being used as adsorbents. Brick particles were then separated by sieving to achieve the particle size 2–5 mm. Then the samples were subjected to calcination in an oven at 105 °C for 24 h. The soaked brick particles were stirred in 1 mol/L sulfuric acid for 3 days to remove impurities from the brick surface and to prevent the excessive pH of the effluent leading to the precipitation of Cu(II). The acid washed bricks were then washed with pure water, dried, and set aside. The Cu(II) solution was prepared by using aqueous solutions of $\text{CuSO}_4 \cdot 5\text{H}_2\text{O}$. Chemicals including NaOH, HNO_3 , and H_2SO_4 were purchased from Sinopharm Chemical Reagent Co., Ltd (Beijing, China).

2.2. Characterization of Bricks

The brick particles were characterized using scanning electron microscopy (SEM, Hitachi Limited S-4800, Tokyo, Japan-SEM) to study the surface morphology. Brunauer–Emmett–Teller (BET, ASAP-2460, Norcross, GA, USA) surface area and Barrett–Joyner–Halenda (BJH) pore size and volume tests were performed on bricks to measure the surface area and porosity. The functional groups on brick were analyzed by Fourier transform infrared spectroscopy (FTIR, Bruker, Germany). The elemental composition of lime sand bricks was determined by X-ray fluorescence (XRF, Shimadzu XRF-1800, Kyoto, Japan).

2.3. Batch Absorption Experiments

The batch experiments were conducted to investigate the adsorption behavior of Cu(II) in lime sand bricks. The experiments were conducted at 25 °C. The adsorption kinetics was studied and adsorption isotherms were measured. All experiments were performed in duplicate. In the adsorption kinetics experiments, 500 mL solutions were prepared with a Cu(II) concentration of 5 mg/L. Brick powders of 2–5 mm were then added into the solution with a dosage of 8 g/L. Solution samples were taken at different time intervals and filtered with 0.45 µm pore diameter nylon micropore membranes. The concentration of Cu(II) in the filtrate was then analyzed by ICP-MS (Elan 5000, Perkin Elmer, Waltham, MA, USA). To measure the adsorption isotherms, a series of 40 mL solutions with a Cu(II) concentration of 0–30 mg/L were prepared. Adsorbents having the same size distribution were then added into the solutions with a dosage of 8 g/L. After reaching equilibrium, the solutions were filtered and the concentration of Cu(II) was analyzed. The pH was controlled using NaOH and HCl to ensure that the pH was around 5.

The data on the adsorption kinetics of Cu(II) were fitted using the pseudo-first-order (Equation (1)) and pseudo-second-order models (Equation (2)).

$$q_t = q_e(1 - e^{-k_1 t}) \quad (1)$$

$$q_t = \frac{q_e^2 \cdot k_2 \cdot t}{1 + q_e \cdot k_2 \cdot t} \quad (2)$$

where k_1 (h^{-1}), k_2 ($\text{g}/\text{mg}\cdot\text{h}$) are the rate constants of adsorption, q_e (mg/g) is the adsorption capacity at equilibrium and q_t is the amount of metal adsorbed at time t (h).

Different models were used to correlate and compare experimental adsorption data to provide an accurate fit of the adsorption isotherms. In this study, the Freundlich and Langmuir isotherm models were used to fit the adsorption isotherms. The Freundlich and Langmuir models are shown in Equations (3) and (4).

$$q_e = K_F \cdot C_e^{1/n} \quad (3)$$

$$q_e = \frac{q_m \cdot K_L \cdot C_e}{1 + K_L \cdot C_e} \quad (4)$$

where q_m (mg/g) is the maximum adsorption capacity of the materials; K_F ($(\text{mg}/\text{g}) (\text{L}/\text{mg})^n$) and K_L (L/mg) are the constants for the Freundlich and Langmuir models, respectively; C_e (mg/L) is the metal concentration in solution at equilibrium; n is a dimensionless empirical parameter, which gives information on the strength of the adsorption.

To investigate the effect of ionic strength on adsorption, 40 mL of a Cu(II) solution with an initial concentration of 5 mg/L was added to each centrifuge tube. The pH was controlled at 5 using NaOH and HCl. The lime sand bricks with a particle size of 0.5–1 mm were added to the solution, and the solid-liquid ratio was 8 g/L. Sodium chloride was used to adjust different levels of ionic strength (i.e., 0, 0.2, 1, 5, 10, 20, 50, 100 and 200 mg/L). All samples were shaken at 135 rpm.

2.4. Column Set-Up

The experimental setup is shown in Figure 1. The experimental columns were employed to investigate the effects of inlet concentration, residence time, and heights on the removal of Cu(II). In order to simulate the use of lime sand bricks for the packing in the percolation facility, the plexiglass columns were employed with a size of 3 cm diameter and 20 cm height. The selected column height fits the design regulations of a permeable pavement by sponge city construction guide in China. In order to avoid sidewall effects as much as possible, the solution was injected from the bottom of the column using a peristaltic pump. Samples were taken at 5 cm, 10 cm, 15 cm, and 20 cm from the bottom of the column to investigate the removal of Cu(II) at different heights. Glass wool is added to each side of the columns to improve the flow rate of the water and prevent the loss of the adsorbent during the process. The quality of each pillar filled lime sand bricks was 195 g. The packing density was calculated to be $1.38 \text{ g}/\text{cm}^3$ based on the filling quality of the brick and the column size. The column porosity is achieved by controlling the flow rate of the peristaltic pump with a porosity of 50.03%. Water samples were collected from different outlets at different time intervals. The columns study was carried out at 25°C . In order to ensure the exclusivity of the adsorption process, the pH of the metal solution was kept below the precipitation pH of the metal. Therefore, the pH of the initial solution was controlled to 2 by the addition of hydrochloric acid, which could ensure the pH of the effluent in the range of 5 to 6. The breakthrough curves and efficiency parameters for evaluating the adsorption performance of the fixed bed were obtained from the experimental data.

$$q = \frac{V(C_0 - C_t)}{m} \quad (5)$$

$$q_t = \frac{60C_0 \cdot Q}{1000m} \int_0^\infty \left(1 - \frac{C_t}{C_0}\right) dt \quad (6)$$

where q (mg/g) is the adsorption capacity per unit mass of construction wastes at any one time; q_t (mg/g) is the adsorption capacity per unit mass of construction wastes; V (L) is the volume of sample; C_0 (mg/L) is the concentration of inlet Cu(II); Q (mL/min) is the inflow rate of the solution; m (g) is the adsorbent quality; C_t (mg/L) is the outlet concentration over a certain period of time.

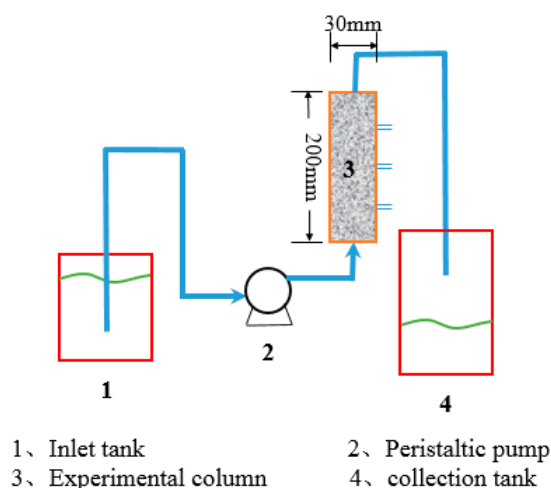


Figure 1. The schematic diagram of the experimental setup.

2.5. The Effect of Bed Depth, Inlet Concentration and Residence Time

To evaluate the effect of bed depth, the height of the filled lime sand bricks was measured at 5, 10, 15 and 20 cm. A Cu(II) solution of 0.5 mg/L was added to the column at a flow rate corresponding to a residence time of 10 min. Samples were taken at different time intervals and filtered through a 0.45 μm membrane filter. A small amount of nitric acid was then added to the sample and stored in the fridge at 0–4 $^{\circ}\text{C}$ before analysis. The inlet concentration was determined according to the drinking water standards in China; the residence time and the height were designed based on the permeability of the permeable pavement and the height of the paving.

To examine the inlet concentration effect on the removal of Cu(II), the concentration of Cu(II) at 0.5, 1.0 and 2.0 mg/L were selected. The residence time of the influent was controlled at 10 min and the bed height was maintained at 20 cm. To study the effect of residence time on the removal of Cu(II), a residence time of 8, 10 and 12 min were selected. The inlet concentration of Cu(II) remained as 0.5 mg/L and the bed height was packed at 20 cm. The effluent was collected for metal analysis at different time intervals.

2.6. Response Analysis by Box–Behnken Design (BBD)

Response surface methodology (RSM) is a useful statistical tool for the optimization of different processes and widely used for experimental design. In this study, the optimization of experimental conditions for the removal of Cu(II) by lime sand bricks was conducted using Box–Behnken design (BBD) technique under RSM. In order to evaluate the removal effects of lime sand bricks on Cu(II), three main factors were chosen: height (cm) (X_1), concentration (mg/L) (X_2) and residence time (min) (X_3). The experimental range and levels of design are shown in Table 1.

Table 1. The experimental range and levels of design of the experiment.

Factor	Variables	Coded Levels of Variables		
		−1	0	1
X_1	Height (cm)	10	15	20
X_2	Concentration (mg/L)	0.5	1.0	2.0
X_3	Residence time (min)	8	10	12

2.7. Adam–Bohart Model

The Adam–Bohart model describes the relationship between C_t/C_0 and t during continuous operation and is usually used to describe the inlet part of the breakthrough curve [18]. The simplified form of the Adam–Bohart model used in this study is referred to as the bed depth service time

(BDST) [19]. The BDST model is used for the interpretation of the inlet part of the breakthrough curve that is up to 10–50% of the breakthrough. The BDST Equation (7) below shows a linear relationship between bed height and breakthrough time, often called service time at the bed.

$$t = \frac{N_0 Z}{C_0 \theta} - \frac{1}{K_a C_0} \ln\left(\frac{C_0}{C_b} - 1\right) \quad (7)$$

where t is the service time at the breakthrough point (hour); N_0 is the adsorption capacity per volume of the bed (mg/cm^3); Z is the depth of the adsorbent bed (cm); C_0 is the influent or inlet solute concentration (mg/L); θ is the linear flow rate (cm/h); K_a is the rate constant of adsorption ($\text{L}/\text{mg}\cdot\text{h}$) and C_b is the effluent concentration at the breakthrough point (mg/L).

2.8. Analytical Methods of Cu(II) and its Sequential Extraction

The procedure proposed by Tessier et al. was applied in this study to analyzed different copper species that was usually used to determine the fractionation of heavy metals in soil and sediment samples [20]. The Cu(II) of the five fractions were analyzed, including the exchangeable fraction, carbonates fraction, Fe-Mn oxides fraction (the fraction associated with Fe and Mn oxides), organic matter fraction (the fraction bound to organic matter) and a residual fraction. After the completion of the experimental column, lime sand bricks were taken out and the Cu(II) adsorbed to bricks were analyzed through sequential extraction in order to distinguish different species. The analysis was carried out for the brick flows through different inlet concentration of 0.5, 1.0 and 2.0 mg/L with a residence time of 10 min. The bricks were baked at 105 °C for 24 h until dry, ground with a mortar and then passed through a 200-mesh screen.

Step 1: exchangeable fraction (F1). The solid samples (2 g) were introduced into three 50 mL centrifuge tubes containing a 16 mL magnesium chloride solution (1 mol/L, adjusted to pH 7 with HNO_3 and NaOH) and shaken for 1 h at 25 °C, respectively. The solution was separated from the solid by centrifugation at 4000 rpm for 20 min. The liquid supernatant was then filtered through a 0.45 μm membrane filter. The solid residue was retained for subsequent analysis.

Step 2: carbonates fraction (F2). A 16 mL volume of sodium acetate solution (1 mol/L, adjusted to pH 5 with HNO_3) was added to the residue from step 1 in a centrifuge tube, which was shaken for 8 h at 25 °C. The solution was separated from the solid by centrifugation at 4000 rpm for 20 min. The extraction procedure depicted above was followed.

Step 3: Fe-Mn oxides fraction (F3). A 16 mL volume of hydroxylamine hydrochloride solution (0.04 mol/L, adjusted to pH 2 with HNO_3) to 25% acetic acid solution in acetic acid solution was added to the residue from step 2, which was shaken for 4 h at 95 ± 2 °C. The solution was separated from the solid by centrifugation at 4000 rpm for 20 min. The extraction procedure depicted above was followed.

Step 4: organic matter fraction (F4). A 5 mL volume of hydrogen peroxide (30%) and 3 mL nitric acid (0.01 mol/L) were added to the residue from step 2. The mixture is heated to 85 °C in a water bath and kept at 85 °C for 2 h with occasional manual stirring. A second 5 mL volume of hydrogen peroxide (30%, adjusted to pH 2 with HNO_3) was introduced and digested at 85 ± 1 °C for 2 h in a water bath. After that, 5 mL of 3.2 mol/L ammonium acetate (adjusted to pH 2 with HNO_3) was introduced to the cooled-down residue, which was then shaken for 0.5 h at 25 °C. Finally, the extract was separated according to the procedure described in step 1.

Step 5: residual fraction (F5). We used the same method as determining the total concentration of heavy metals in the sample. The residue from the metal content of step 3 was digested with 10 mL of aquaregia heated on a heater and then evaporated to near dryness according to ISO recommendations. After cooling down, the residues were diluted in 50 mL 5% HNO_3 .

In order to determine the total concentration of Cu(II) in the top layer of the lime sand bricks in the column, the lime sand bricks were used for digestion by microwave digestion.

A total of 0.1 g of brick sample was weighed into a poly tetra fluoro ethylene digestion tank, and a blank sample of 0.1 mL of ultrapure water was used instead of the brick sample in one digestion

tank. A total of 5 mL volume of nitric acid, 2 mL volume of hydrogen peroxide and 3 mL volume of hydrofluoric acid were sequentially added to the digestion tank. After cooling, the solution was transferred to a polytetrafluoroethylene crucible, and heated at 130 °C on a hot plate to catch the acid to a viscous state. After removing the crucible, the samples were transferred to 100 mL volumetric flask and dilute to the mark with water.

The solution concentrations before and after the adsorption process were determined by ICP-MS.

3. Results and Discussion

3.1. Characterization of the Lime Sand Bricks

The specific surface area of the brick determined using the BET method is 1.75 m²/g with an average pore size of 12.00 nm and the total pore volume on the brick was 0.0051 cm³/g. The surface area of bricks was a bit higher compared to chitosan of 1.05 m²/g [21] and perlite of 1.66 m²/g [22]. This property provides a larger surface area for the lime sand bricks, providing more active adsorption sites for adsorption. The surface topography of the brick was analyzed by SEM, as shown in Figure 2. It was observed that the surfaces of lime sand bricks were uneven with large numbers of pore spaces, which perhaps provided sites for adsorption of Cu(II) either physically or chemically [23]. Figure 3 shows the FTIR spectra of the lime sand brick before Cu(II) adsorption. The bands at 1444 cm⁻¹ before adsorption was assigned to the O-H bending vibration of lime sand bricks [24]. The peaks at 2520 cm⁻¹ for lime sand bricks before adsorption can be assigned to -C=OH-OH [25]. The bands in the range 729–877 cm⁻¹ may be assigned to the -C=CH₂ double bonds [26]. The bands in the range 1010–1092 cm⁻¹ can possibly be assigned to the -C=O-O- bond [27]. Studies have shown that carboxyl (-COOH), hydroxyl (-OH) and phenol (R-OH) can coordinate with heavy metal ions such as Cu²⁺ [28]. Table 2 shows the elemental composition of the lime sand bricks, which mainly consisted of CaO, SiO₂, MgO, Al₂O₃ and Fe₂O₃. The content of CaO was the largest among all elements (42.16%). Calcium and magnesium are exchangeable cations allowing for its exchange with Cu(II), which could have a positive effect on Cu(II) adsorption.

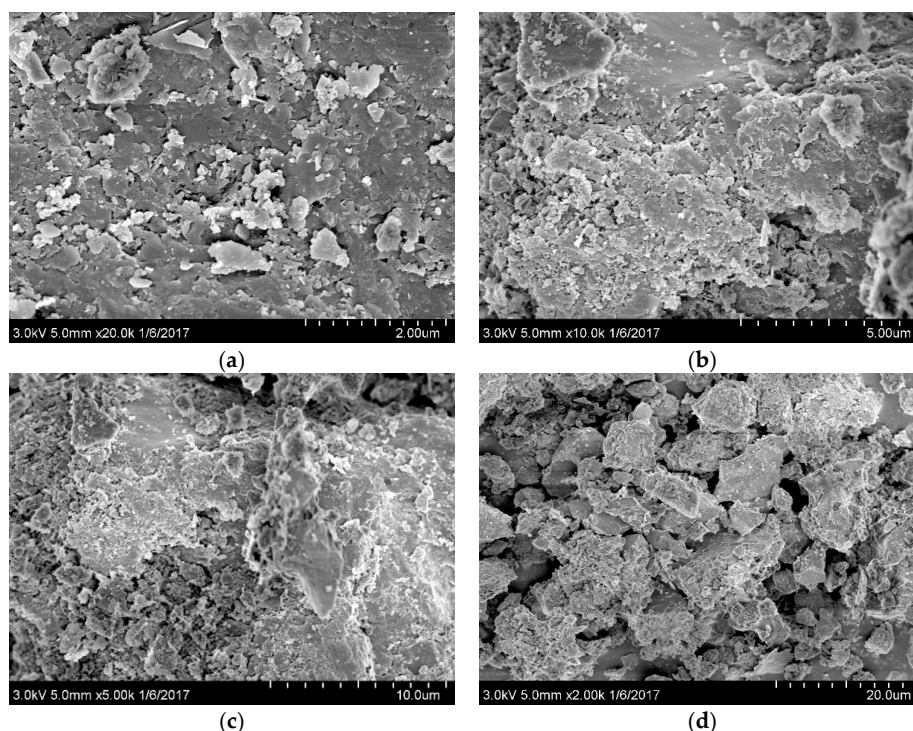


Figure 2. The scanning electron microscopy (SEM) image of lime sand bricks observed at different scales. (a) 2.00 μm; (b) 5.00 μm; (c) 10.0 μm; (d) 20.0 μm.

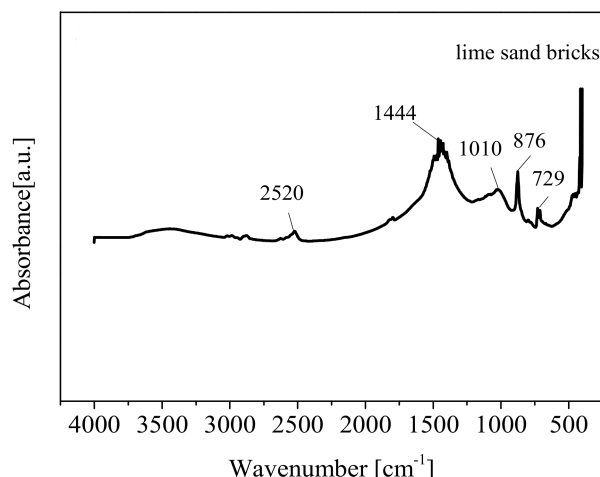


Figure 3. The Fourier transform infrared spectroscopy (FITR) spectra of lime sand bricks.

Table 2. The major elements’ contents (oxide%) in lime sand bricks measured by X-ray fluorescence (XRF).

Composition	MgO	Al ₂ O ₃	SiO ₂	CaO	MnO	Fe ₂ O ₃	P ₂ O ₅	Others
Content (%)	4.92	3.93	15.74	42.16	0.02	0.67	0.02	32.54

3.2. Batch Absorption Experiments

3.2.1. Adsorption Kinetics of Cu(II) into Lime Sand Bricks

For investigation of the adsorption kinetics of Cu(II) with brick particles, it is important to monitor how fast the interaction takes place [29]. Figure 4 shows the kinetic behavior of Cu(II) uptake by the lime sand bricks. Under the conditions (i.e., $C_0 = 5 \text{ mg/L}$, solid-liquid ratio = 8 g/L, stirring speed = 135 rpm, pH = 5), the adsorption of Cu(II) onto the lime sand bricks reached an equilibrium within 7 h. It is apparent that the adsorption is fast at the initial stage and then reaches a plateau, indicating that adsorption equilibrium is reached. Initially, the removal is fast due to the adsorption of Cu(II) ions onto the vacant surface sites, and thereafter the rate decreases due to the saturation of the surface sites [30].

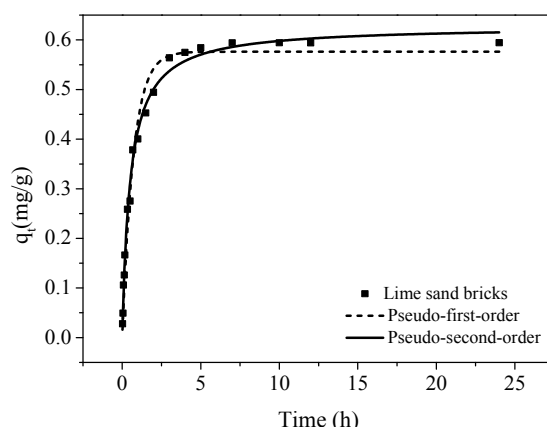


Figure 4. The kinetics of Cu(II) removal by lime sand brick bricks at 25 °C ($C_0 = 5 \text{ mg/L}$, solid-liquid ratio = 8 g/L, stirring speed = 135 rpm, pH = 5).

The adsorption kinetic data were fitted by pseudo-primary-order and pseudo-second-order models. Table 3 shows the parameters obtained from these two models. It can be concluded that the adsorption kinetics of Cu(II) on lime sand bricks is more in line with the pseudo-second-order model ($r^2 > 0.99$) because the fitting obtains a higher r^2 . This indicates that the adsorption follows the pseudo-second-order model. The model is based on the assumption that the rate-limiting phase can be

described by chemisorption, which involves the valence of electrons shared or exchanged between the adsorbent and the adsorbate [28]. The current results are consistent with Boujelben et al. who observed that the adsorption of Pb(II) on manganese oxide coated bricks conforms to the pseudo-second-order model [31]. Zhang et al. observed that the adsorption of Zn(II) by lime sand bricks is also in accordance with the pseudo-second-order kinetics model [26]. The rapid metal uptake was clearly related to the availability of active sites on the bricks surfaces [26].

Table 3. The parameters deduced by pseudo-first and pseudo-second-order models for the adsorption of Cu(II) by lime sand bricks.

Models	Pseudo-First-Order			Pseudo-Second-Order		
	q_e (mg/g)	k_1 (min ⁻¹)	r^2	q_e (mg/g)	k_2 (g/mg·min)	r^2
lime sand bricks	0.58 ± 0.01	1.41 ± 0.11	0.97	0.63 ± 0.01	3.13 ± 0.22	0.99

3.2.2. Adsorption Isotherms of Cu(II) onto Lime Sand Bricks

Two of the most commonly used isotherm equations, Langmuir and Freundlich [32], were chosen to fit the adsorption isotherms of Cu(II) onto lime sand bricks. The values of the derived isotherm parameters are listed in Table 4 along with the r^2 of the fits. Both the Langmuir and Freundlich models fit well with Cu(II) adsorption by lime sand bricks (Figure 5). The Langmuir model shows slightly larger r^2 than the Freundlich model. We chose the Langmuir model to obtain the maximum adsorption capacity of the lime sand bricks. Many previous studies have used this model to describe the adsorption of heavy metals on heterogeneous adsorbents such as bricks and bentonite [33], red clay stone [5] and zeolite [34]. The adsorption capacity and affinity of lime sand bricks for Cu(II) were evaluated by analyzing the parameters q_m and K_L of the Langmuir equation (Table 4). The maximum adsorption capacity of the lime sand bricks was 7.01 mg/g.

Table 4. The parameters of Langmuir and Freundlich isotherms for the adsorption of Cu(II) by lime sand bricks.

Models	Langmuir Model			Freundlich Model		
	q_m (mg/g)	K_L (L/mg)	r^2	K_F (mg/g) (L/mg) ⁿ	n	r^2
lime sand bricks	7 ± 1	0.04 ± 0.01	0.99	0.39 ± 0.07	1.39 ± 0.14	0.97

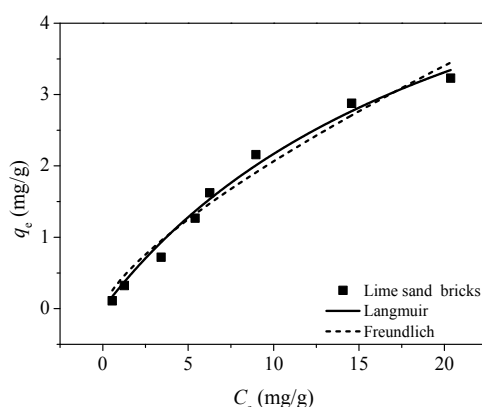


Figure 5. The adsorption isotherms of Cu(II) by lime sand bricks at 25 °C (solid-liquid ratio = 8 g/L, stirring speed = 135 rpm, pH = 5).

From the elemental analysis, the lime sand bricks contain more exchangeable cations, which are beneficial to the occurrence of ion exchange. In addition, we measured the cation exchange capacity and found that the cation exchange capacity in the lime sand bricks was 46.67 mmol/g, which also

facilitated the occurrence of ion exchange. Therefore, it was considered that the adsorption of Cu(II) by lime sand bricks was mainly the role of ion exchange.

Table 5 presents a comparison of Cu(II) adsorption capacity for different types of natural adsorbents. Among the listed natural adsorbents, The adsorption capacity of bricks for Cu(II) adsorption is slightly larger than some low-cost adsorbents such as fly ash [35–37] and zeolite [38,39], while the capacity of bricks is smaller than the traditional adsorbents such as cedar sawdust [40] and clays [41]. As waste materials, bricks could still be applied as adsorbents or filling materials in some filtration devices such as in a permeable pavement to remove pollutants due to their large adsorption capacities and low cost. In the process of adsorption of copper on bricks, both physical adsorption and ion exchange play a very important role.

Table 5. The adsorption capacity of the adsorbent for copper in water treatment.

Adsorbent	q_m (mg/g)	References
Lime sand bricks	7.01	this study
Limestone	0.0145	[42]
Cedar sawdust	29.84	[40]
Clinoptilolite	1.64	[38]
Zeolite	5.10	[39]
Clays	9.58	[41]
Fly ash	1.39	[35]

3.2.3. Effect of Ionic Strength

The effect of ionic strength (0–200 mg/L) on the absorption of Cu(II) by lime sand bricks was studied (Figure 6). The results indicate that at lower sodium chloride concentrations (i.e., 0–5 mg/L), the adsorption of Cu(II) by lime sand bricks decreased with increasing salt concentration, with the adsorption capacity decreasing from 0.59 mg/g to 0.56 mg/g. With the increase of NaCl concentration from 5 mg/g to 20 mg/L, the adsorption of Cu(II) increased rapidly from 0.56 mg/g to 0.62 mg/g. As the ionic strength further increases, the adsorption capacity of lime sand bricks to copper increases slowly. Ion exchange was suggested to be the main mechanism in the adsorption process. The initial depression of Cu(II) adsorption by ionic strength might be due to the competition of Na⁺ ions with Cu cations for the same binding sites on the sorbent surface [40,43]. The adsorption of Cu(II) was then increased with the increase of salt concentration, which can be explained by the fact that sodium chloride acts as an in situ regenerating agent for the sorbent via removal of oxygenated complexes as soluble chlorine complexes, thereby increasing the number of adsorption sites and, hence, the adsorption of the Cu(II) species [40].

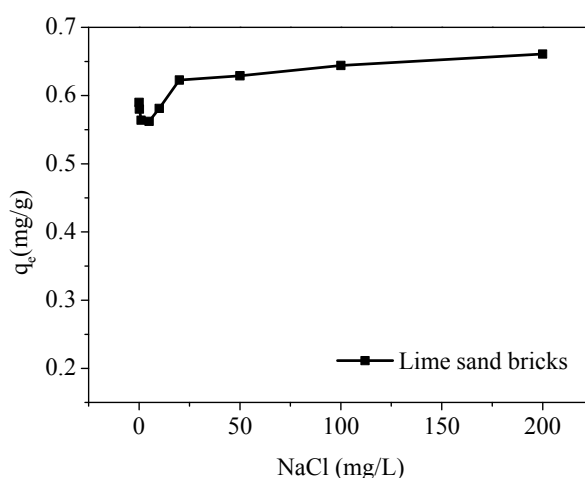


Figure 6. The effect of ionic strength (NaCl) on the adsorption of copper from aqueous solution by lime sand bricks at 25 °C ($C_0 = 5$ mg/L, solid-liquid ratio = 8 g/L, stirring speed = 135 rpm, pH = 5).

3.3. The Influence of Operating Parameters on Column Sorption

3.3.1. The Effect of Bed Depth on Cu(II) Removal

The effect of varying bed depth (5, 10, 15, 20 cm) on breakthrough curves at a constant residence time of 10 min and inlet Cu(II) concentration was 0.5 mg/L and the results are shown in Figure 7. The results indicate that the breakthrough times increased with the increase of bed depth. The breakthrough times were 0.78 h, 2.69 h, 4.99 h and 7.35 h for 5 cm, 10 cm, 15 cm and 20 cm bed depths, respectively. The bed exhaustion time increased from 45.76 h to 154.92 h with the bed depth increase from 5 cm to 20 cm. This may be due to the adsorption of more binding sites at higher bed depths to obtain adsorption, resulting in a higher number of mass transfer zones [44]. Therefore, one can assume that more wastewater can be treated at a higher bed depth, while a higher percentage of metal can be removed. On the other hand, a smaller bed depth gets saturated in a shorter time which results in a shorter breakthrough time. Therefore, it can be concluded that as the bed depth increases, the increase in Cu(II) absorption in the column is due to an increase in contact time with the bricks. The adsorption capacity of the bricks increased from 75.57 mg/kg to 83.98 mg/kg with the bed depth increase from 5 cm to 20 cm. A length of 20 cm was chosen as the optimum bed depth for further experiments.

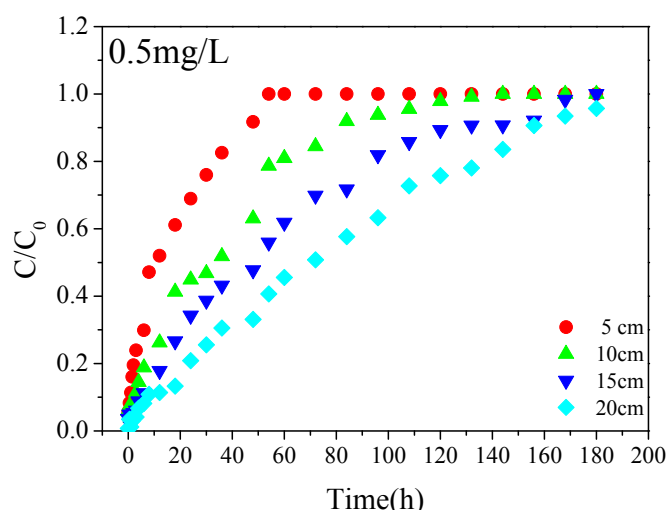


Figure 7. The breakthrough curve for varying bed depth (cm) at a residence time of 10 min and 0.5 mg/L inlet Cu(II) concentration.

3.3.2. The Effect of Inlet Concentration on Cu(II) Removal

The effect of inlet Cu(II) concentration (0.5, 1.0 and 2.0 mg/L) on the penetration curve performance for a constant bed depth (20 cm) and a 10 min residence time is shown in Figure 8. The breakthrough time (t_b) decreased with the increase of inlet Cu(II) concentration (t_b was 7.35 h, 1.24 h and 0.18 h for inlet Cu(II) concentration of 0.5, 1.0 and 2.0 mg/L, respectively). The exhaustion time (t_e) decreased from 154.92 h (0.5 mg/L) to 118.61 h (2.0 mg/L) with the inlet Cu(II) concentration increasing from 0.5 mg/L to 2.0 mg/L. The adsorption capacity increased from 87.75 mg/kg to 169.59 mg/kg with the increase of the Cu(II) concentration from 0.5 mg/L to 2.0 mg/L. The breakthrough point refers to the point where C/C_0 is 0.1, and the exhaustion point refers to the point where C/C_0 is 0.9. At a low inlet Cu(II) concentration, the breakthrough curves occurred later and the treated volume of the outlet was higher resulting in higher breakthrough time. This may be due to the fact that the lower concentration gradient resulted in slower transport due to the reduced diffusion coefficients [45]. whereas, at higher inlet Cu(II) concentrations, the adsorbent gets saturated early because the binding sites become more quickly saturated in the column, resulting in an earlier breakthrough and exhaustion time.

Under the same concentration, the comparison of sorption capacity in the batch system and column system is shown in Table 6. The adsorption capacity obtained from the dynamic experiment

is smaller than the adsorption capacity obtained from the static experiment. As the concentration increases, the ratio of the static adsorption capacity to the dynamic adsorption capacity gradually decreases. This may be due to the fact that the adsorption is particularly active in the dilute concentrations. Demey et al. and Kleinübing et al. also observed a higher sorption capacity obtained from the batch experiment than from the column experiments [46,47]. The fact was explained by the resistance to the film diffusion active in the low concentrations which are similar to the present study. In addition, the removal of Cu(II) could be improved by reducing the flow rate.

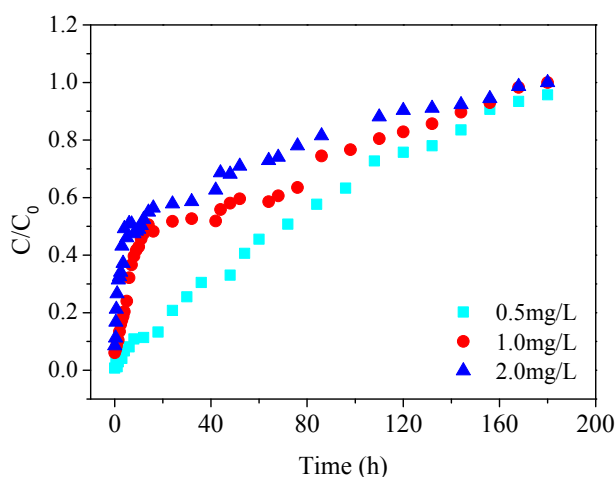


Figure 8. The breakthrough curve for varying inlet concentration (mg/L) at a bed depth of 20 cm and a residence time of 10 min.

Table 6. The comparison of sorption capacity obtained from the batch system and column system.

Initial/Inlet Concentration		0.5 mg/L	1.0 mg/L	2.0 mg/L
sorption capacity	batch system	0.098 mg/g	0.114 mg/g	0.1775 mg/g
	column system	0.088 mg/g	0.104 mg/g	0.1696 mg/g
ratio	$\frac{\text{Sorption capacity—Batch}}{\text{Sorption capacity—Column}}$	1.101	1.096	1.046

3.3.3. The Effect of Residence Time on Cu(II) Removal

The effect of residence time was investigated by varying residence time (8, 10 and 12 min) at a constant bed depth (20 cm) and a constant Cu(II) concentration of 0.5 mg/L. The breakthrough curve of C/C_0 versus time with varying residence time is shown in Figure 9. The results indicated that increasing the residence time at a constant bed depth increased breakthrough time (t_b). The breakthrough times were 2.05 h, 6.98 h and 15.10 h at residence times of 8, 10 and 12 min, respectively. The bed exhaustion time (t_e) decreased from 174.04 h to 134.23 h with the residence time decreasing from 12 min to 8 min. With a shorter residence time, the contact between Cu(II) and the lime sand bricks was quicker, thus, the diffusion of copper ions into brick pores is insufficient. When the residence time of solution is shorter in the column, the equilibrium is not reached, therefore, Cu(II) solution leaves column before reaching equilibrium. On the other hand, a higher residence time allows Cu(II) to diffuse and reach the active sites of the sorbent. The finding is in agreement with the results obtained by Demey et al. on neodymium removal using the low cost composite material of chitosan/Iron(III) hydroxide [ChiFer(III)] [46], who conclude that the external film diffusion reduced under the higher superficial velocity, thus, resulting in a faster breakthrough. The Cu(II) adsorption capacity was 59.65, 84.98 and 98.16 mg/kg with the increasing residence times for 8, 10 and 12 min, respectively. These results may be considered that Cu(II) adsorption in lime sand bricks columns requires longer contact times and lower flow rates.

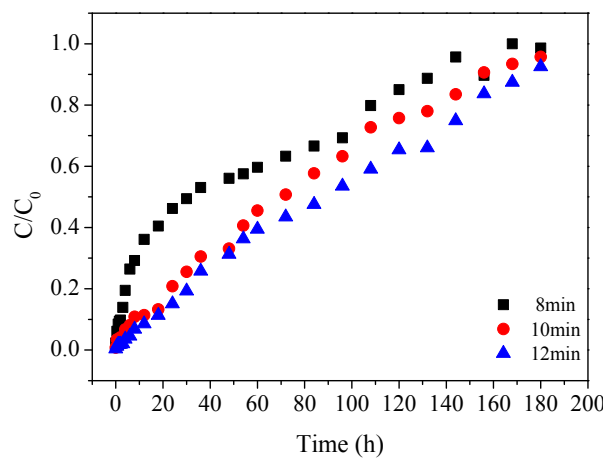


Figure 9. The breakthrough curve for varying residence time (min) at a bed depth of 20 cm and inlet Cu(II) concentration of 0.5 mg/L.

Compared with the adsorbent such as activated carbon, although the adsorption capacity is much different, the construction waste bricks are used as a kind of garbage for treating heavy metals in the aqueous solution, and the effect of wastes treatment can be achieved. Moreover, the activated carbon resources are limited, the lifespan is short, and the cost of regeneration operations is high. Compared with other adsorbents, such as biomass, gravel, zeolite, etc., although the adsorption capacity of construction wastes bricks is relatively low, the amount of construction wastes is large and with large economic advantages.

3.4. Response Analysis and Interpretation by Box–Behnken Design (BBD)

The design matrix of the variables (height, X₁; concentration, X₂ and residence time, X₃) in the uncoded and coded units by the Box–Behnken design (BBD) are shown in Table 7, along with the predicted and experimental values of the responses (adsorption capacity, Y). The response function with the determined coefficients for adsorption capacity of lime sand bricks towards Cu(II) is presented by Equation (8).

$$Y = 0.1034 - 1.512 \times 10^{-3}A + 0.0194B + 0.0112C - 1.825 \times 10^{-3}AB - 3.2 \times 10^{-3}AC - 5.225 \times 10^{-3}BC - 5.45 \times 10^{-4}A^2 - 6.67 \times 10^{-3}B^2 - 0.0117 \times C^2 \tag{8}$$

Table 7. The experimental design matrix and response based on the experimental runs by Box–Behnken Design (BBD).

Run	Variables			Response (Y, mg/g)	
	Height (cm)	Concentration (mg/L)	Residence Time (min)	Experimental Adsorption Capacity	Predicted Adsorption Capacity
1	0	0	0	0.1034	0.1026
2	0	0	0	0.1034	0.1031
3	0	1	1	0.1209	0.1139
4	1	-1	0	0.0840	0.0771
5	0	1	-1	0.1009	0.0985
6	-1	-1	0	0.0826	0.0765
7	0	0	0	0.1034	0.1034
8	0	0	0	0.1034	0.1034
9	0	-1	1	0.0796	0.0820
10	-1	0	1	0.1034	0.1071
11	0	-1	-1	0.0387	0.0492
12	1	1	0	0.1062	0.1123
13	-1	0	-1	0.0827	0.0783
14	1	0	-1	0.0853	0.0817
15	1	0	1	0.0932	0.0976
16	-1	1	0	0.1121	0.1190
17	0	0	0	0.1034	0.1034

The analysis of variance (ANOVA) tests were also conducted for each response and presented in Table 8. It is indicated that the predictability of the model is at a 90% confidence level. Response function predictions agreed well with the experimental data ($r^2 = 0.914$). To evaluate the relationship between the predicted values from the model calculated by Equation (3) and the observed values, the data obtained was very close to linear, indicating that both values were accurate and reliable, as shown in Figure 10.

Table 8. The analysis of variance (ANOVA) results for the adsorption capacity of lime sand bricks towards Cu(II) (mg/g).

Source	Sum of Squares	Mean Square	F Value	p-Value Prob > F
Model	5.009×10^{-3}	5.566×10^{-4}	8.34	0.0053
X ₁	1.830×10^{-5}	1.830×10^{-5}	0.27	0.6166
X ₂	3.011×10^{-3}	3.011×10^{-3}	45.13	0.0003
X ₃	1.001×10^{-3}	1.001×10^{-3}	15.01	0.0061
X ₁ X ₂	1.332×10^{-5}	1.332×10^{-5}	0.2	0.6685
X ₁ X ₃	4.096×10^{-5}	4.096×10^{-5}	0.61	0.4590
X ₂ X ₃	1.092×10^{-4}	1.092×10^{-4}	1.64	0.2416
X ₁ ²	1.251×10^{-6}	1.251×10^{-6}	0.019	0.8590
X ₂ ²	1.873×10^{-4}	1.873×10^{-4}	2.81	0.1377
X ₃ ²	5.808×10^{-4}	5.808×10^{-4}	8.71	0.0214
Residual	4.670×10^{-4}	6.672×10^{-5}	-	-
Lack of Fit	4.670×10^{-4}	1.557×10^{-4}	19459.06	<0.0001
Pure Error	3.200×10^{-8}	8.000×10^{-9}	-	-
Cor Total	5.477×10^{-3}	-	-	-

$r^2 = 0.914$, Adjust $r^2 = 0.905$

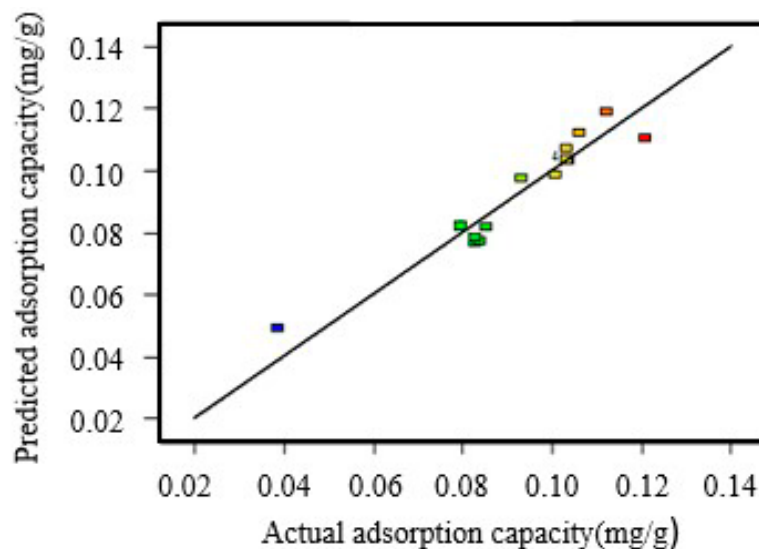


Figure 10. The regression plots of the actual data against the predicted values from the response surface models describing.

It is required to test the significance and adequacy of the model through the analysis of variance. The F-value indicates that the factors adequately explain the variation in the data about its mean, and the estimated factor effects are real. The corresponding analysis of variance (ANOVA) is presented in Table 8. Concentration (X₂) and residence time (X₃) in the model have significant effects on the amount of adsorption since the p-value was less than 0.05.

3.5. Adams-Bohart Model

Iso-removal lines show the time versus bed depth (Figure 11) under constant experimental conditions except for bed depth (residence time of 10 min, inlet Cu(II) concentration of 0.5 mg/L). The BDST model was used to determine the efficiency of lime sand bricks in column mode. It is based on measuring the capacity of a fixed bed column at different breakthrough values and predicting the relationship between bed depth and time [47]. This relationship can be used to calculate the adsorptive capacity (N_0) which represents the time required for the adsorption zone to move through the adsorbent per unit length. The Adams-Bohart constant which characterizes the net effect of mass transfer in the liquid and solid phase, can also be evaluated from the equation. The main parameters of the BDST equation are sorption capacity, N_0 (mg/L) and rate constant of adsorption, K_a (L/mg·h) which characterizes that the rate of solute transfer from the liquid phase to the solid phase can be calculated from the slope and intercept of the respective lines (Table 9). The BDST curve was linear with a high correlation coefficient (>0.95) of Cu(II) indicating the validity of the BDST model of the present system. The values of N_0 and K_a suggested that lime sand bricks have a high efficiency for the removal of Cu^{2+} from an aqueous solution. The equation of the BDST model (Equation (5)) enables the service time of the sorption bed for a specified bed depth of the adsorbent to be determined. The service time and bed depth are related to the process parameters such as inlet concentration, solution residence time and sorption capacity.

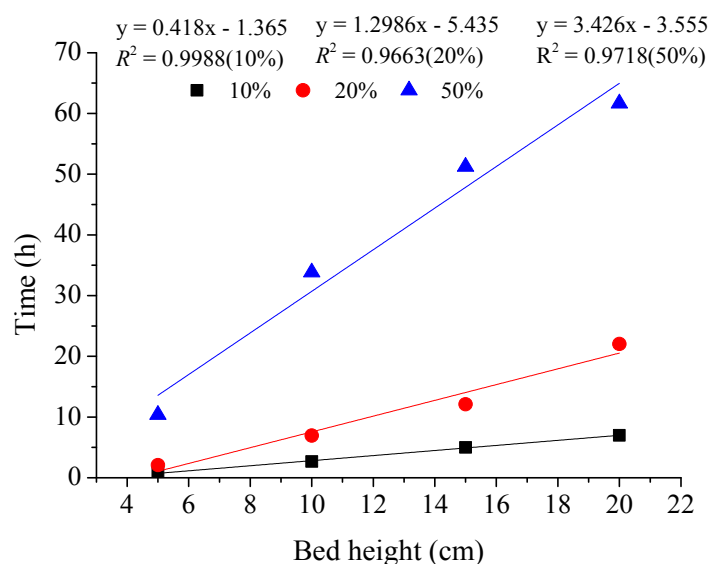


Figure 11. The Adams-Bohart model for 10%, 20% and 50% breakthrough levels at different bed depths and a constant inlet concentration (0.5 mg/L) and residence time (10 min).

Table 9. The Adams-Bohart model constants for the adsorption of Cu(II) in lime sand bricks.

Iso-Removal Percentage (%)	N_0 (mg/L)	K_a (L/mg·h)	r^2
10	25.08	3.22	1.00
20	77.92	0.51	0.97
50	205.56	0.00	0.97

3.6. Fractionation of Copper in Lime Sand Brick and Total Concentration

Five different chemical forms of copper in lime sand bricks samples were extracted and morphologically analyzed. Table 10 shows the content of copper in lime sand bricks at different inlet concentrations and the chemical speciation distributions of copper in lime sand bricks. The copper fractions in bricks descend in the following order: organic matter fraction > Fe-Mn oxides fraction > carbonates fraction > residual fraction > exchangeable fraction. Different inlet concentrations showed

the same results. In all samples, copper had the least amount of exchangeable fractions (3.3–5.6 mg/kg). As the inlet concentration increases, the content of different forms of copper increases. It shows that with the increase of the concentration of copper, the removal effect of the lime sand brick on copper also improved. It is well known that copper preferably combines with organic matter. In this study, about 35–38% of total Cu was contained in this fraction in the lime sand bricks (Table 10). The high stability of Cu-organic matter complexes was also reported by Yuan et al [48]. The vast majority of the residual fraction of Cu can be enclosed inside the crystal structure and would not be easily absorbed by the organism., thus, the environmental risk is small [49]. The sum of the proportions of F4 and F5 was between 50% and 60%. The results showed that the lime sand bricks after copper adsorption reduce the long-term ecotoxicity and bioavailability to the environment. By microwave digestion of lime sand bricks with different influent copper concentrations (0.5, 1.0 and 2.0 mg/L), the contents were found to be 69.7 mg/kg, 91.5 mg/kg and 138.0 mg/kg, respectively. This is basically consistent with the results of the sequential extraction analysis.

Table 10. The total concentration and speciation of copper (mg/kg).

Inlet Concentration	Exchangeable Fraction (F1)	Carbonates Fraction (F2)	Fe-Mn Oxides Fraction (F3)	Organic Matter Fraction (F4)	Residual Fraction (F5)	Total	Recovery (%)
0.5	3.3	14.5	11.8	27.2	9.9	69.7	95.7
1.0	4.9	17.2	18.8	35.2	15.6	91.5	100.2
2.0	5.6	19.6	41.8	49.0	17.4	138.0	96.7

$$\text{Recovery} = (\text{F1} + \text{F2} + \text{F3} + \text{F4} + \text{F5}) / \text{Total} \times 100\%.$$

4. Conclusions

The lime sand bricks were systematically investigated as potential filter materials for the removal of Cu(II) from aqueous solutions using static batch experiments and fixed bed continuous column experiments. The study provides basic knowledge on using construction wastes bricks as a potential economical medium for removing heavy metals in the aqueous phase. The conclusions are listed as follows:

(1) The adsorption process revealed that the initial uptake was achieved in 7 h. The isotherm results showed that the amount of Cu(II) adsorbed is large and the maximum adsorption capacity could reach 7.01 mg/g.

(2) Higher bed depths (20 cm) and a longer residence time (12 min) contributed to a more efficient treatment system in the fixed-bed column.

(3) The adsorption capacity of lime sand bricks increased with the increase of inlet concentration. When the inlet concentration was 2.0 mg/L, the adsorption capacity reached at 169.59 mg/kg.

(4) The Box–Behnken design results show that the inlet concentration and residence time in the column experiment have significant effects on the removal of Cu(II) by lime sand bricks. The Adams-Bohart model with a high r^2 (0.99) can predict the change of the effluent concentration with time in the Cu(II) removal process.

(5) The ecotoxicity, bioavailability and mobility of Cu(II) in lime sand bricks depended on their chemical speciation rather than their total concentrations. Sequential extraction showed that the lime sand bricks after adsorption of copper can decrease the ecotoxicity and bioavailability.

Author Contributions: Investigation, K.S.; Methodology, Z.Z.; Resources, C.T.; Validation, J.L. and H.L.; Writing—original draft, S.G.; Writing—review & editing, X.Z.

Funding: This research was supported by the National Natural Science Foundation of the China-Youth Project (51678025); Construction of High Level Teaching Teams in Universities of Beijing—the Youth Top-Notch Talent Cultivation Program (CIT&TCD201804051); the Scientific Research Project of Beijing Educational Committee (SQKM201710016016); the Fundamental Research Funds of Beijing Vocational College of Agriculture; Pyramid Talent Cultivation Project and the Fundamental Research Funds of Beijing University of Civil Engineering and Architecture; Great Scholars Program (CIT&TCD20170313); Beijing Advanced Innovation Center for Future Urban Design: Sponge City Development and Water Quantity & Quality Risk Control (UDC2016040100).

Conflicts of Interest: The authors declare no conflict of interest.

References

1. Wang, J.; Zhang, P.; Yang, L.; Huang, T. Adsorption characteristics of construction waste for heavy metals from urban stormwater runoff. *Chin. J. Chem. Eng.* **2015**, *23*, 1542–1550. [[CrossRef](#)]
2. Ahmad, M.F.; Haydar, S. Evaluation of a newly developed biosorbent using packed bed column for possible application in the treatment of industrial effluents for removal of cadmium ions. *J. Taiwan Inst. Chem. Eng.* **2016**, *62*, 122–131. [[CrossRef](#)]
3. Hamdaoui, O. Dynamic sorption of methylene blue by cedar sawdust and crushed brick in fixed bed columns. *J. Hazard. Mater.* **2006**, *138*, 293–303. [[CrossRef](#)] [[PubMed](#)]
4. Wilson, S.; Newman, A.P.; Puehmeier, T.; Shuttleworth, A. Performance of an oil interceptor incorporated into a pervious pavement. *Eng. Sustain.* **2003**, *156*, 51–58. [[CrossRef](#)]
5. Hussain, S.; Gul, S.; Khan, S.; Rehman, H.-U.; Ishaq, M.; Khan, A.; Jan, F.A.; Din, Z.U. Removal of Cr(VI) from aqueous solution using brick kiln chimney waste as adsorbent. *Desalin. Water Treat.* **2015**, *53*, 373–381. [[CrossRef](#)]
6. Nnadi, E.O.; Newman, A.P.; Coupe, S.J.; Mbanaso, F.U. Stormwater harvesting for irrigation purposes: An investigation of chemical quality of water recycled in pervious pavement system. *J. Environ. Manag.* **2015**, *147*, 246–256. [[CrossRef](#)]
7. Lizama-Allende, K.; Jaque, I.; Ayala, J.; Montes-Atenas, G.; Leiva, E. Arsenic Removal Using Horizontal Subsurface Flow Constructed Wetlands: A Sustainable Alternative for Arsenic-Rich Acidic Waters. *Water* **2018**, *10*, 1447. [[CrossRef](#)]
8. Arsenovic, M.; Radojevic, Z.; Stankovic, S. Removal of toxic metals from industrial sludge by fixing in brick structure. *Constr. Build. Mater.* **2012**, *37*, 7–14. [[CrossRef](#)]
9. Cataldo, S.; Gianguzza, A.; Milea, D.; Muratore, N.; Pettignano, A.; Sammartano, S. A critical approach to the toxic metal ion removal by hazelnut and almond shells. *Environ. Sci. Pollut. Res.* **2017**, *25*, 4238–4253. [[CrossRef](#)]
10. Meena, A.K.; Mishra, G.K.; Rai, P.K.; Rajagopal, C.; Nagar, P.N. Removal of heavy metal ions from aqueous solutions using carbon aerogel as an adsorbent. *J. Hazard. Mater.* **2005**, *122*, 161–170. [[CrossRef](#)]
11. Suksabye, P.; Thiravetyan, P.; Nakbanpote, W. Column study of chromium(VI) adsorption from electroplating industry by coconut coir pith. *J. Hazard. Mater.* **2008**, *160*, 56–62. [[CrossRef](#)] [[PubMed](#)]
12. Kundu, S.; Gupta, A.K. Arsenic adsorption onto iron oxide-coated cement (IOCC): Regression analysis of equilibrium data with several isotherm models and their optimization. *Chem. Eng. J.* **2006**, *122*, 93–106. [[CrossRef](#)]
13. Rajamohan, N.; Sivaprakash, B. Biosorption of heavy metal using brown seaweed in a regenerable continuous column. *Asia-Pac. J. Chem. Eng.* **2008**, *3*, 572–578. [[CrossRef](#)]
14. Vijayaraghavan, K.; Prabu, D. Potential of *Sargassum wightii* biomass for copper(II) removal from aqueous solutions: Application of different mathematical models to batch and continuous biosorption data. *J. Hazard. Mater.* **2006**, *137*, 558–564. [[CrossRef](#)] [[PubMed](#)]
15. Ruiz, M.; Roset, L.; Demey, H.; Castro, S.; Sastre, A.M.; Pérez, J.J. Equilibrium and dynamic studies for adsorption of boron on calcium alginate gel beads using principal component analysis (PCA) and partial least squares (PLS). *Materialwiss. Werkstofftech.* **2013**, *44*, 410–415. [[CrossRef](#)]
16. Fiol, N.; Escudero, C.; Poch, J.; Villaescusa, I. Preliminary studies on Cr(VI) removal from aqueous solution using grape stalk wastes encapsulated in calcium alginate beads in a packed bed up-flow column. *React. Funct. Polym.* **2006**, *66*, 795–807. [[CrossRef](#)]
17. Chu, K.H. Fixed bed sorption: Setting the record straight on the Bohart-Adams and Thomas models. *J. Hazard. Mater.* **2010**, *177*, 1006–1012. [[CrossRef](#)]
18. Kalavathy, H.; Karthik, B.; Miranda, L.R. Removal and recovery of Ni and Zn from aqueous solution using activated carbon from *Hevea brasiliensis*: Batch and column studies. *Colloids Surf. B Biointerfaces* **2010**, *78*, 291–302. [[CrossRef](#)]
19. Simate, G.S.; Ndlovu, S. The removal of heavy metals in a packed bed column using immobilized cassava peel waste biomass. *J. Ind. Eng. Chem.* **2015**, *21*, 635–643. [[CrossRef](#)]
20. Thinh, N.V.; Osanai, Y.; Adachi, T.; Thai, P.K.; Nakano, N.; Ozaki, A.; Kuwahara, Y.; Kato, R.; Makio, M.; Kurosawa, K. Chemical speciation and bioavailability concentration of arsenic and heavy metals in sediment and soil cores in estuarine ecosystem, Vietnam. *Microchem. J.* **2018**, *139*, 268–277. [[CrossRef](#)]

21. Fotalan, C.M.; Kan, C.C.; Dalida, M.L.; Pascua, C.; Wan, M.W. Fixed-bed column studies on the removal of copper using chitosan immobilized on bentonite. *Carbohydr. Polym.* **2011**, *83*, 697–704. [[CrossRef](#)]
22. Petrella, A.; Spasiano, D.; Rizzi, V.; Cosma, P.; Race, M.; De Vietro, N. Lead Ion Sorption by Perlite and Reuse of the Exhausted Material in the Construction Field. *Appl. Sci.* **2018**, *8*, 1882. [[CrossRef](#)]
23. Feng, Y.; Lu, B.; Jiang, Y.; Chen, Y.; Shen, S. Performance evaluation of anaerobic fluidized bed reactors using brick beads and porous ceramics as support materials for treating terephthalic acid wastewater. *Desalin. Water Treat.* **2015**, *53*, 1814–1821. [[CrossRef](#)]
24. Boujelben, N.; Gouider, M.; Elouear, Z.; Bouzid, J.; Feki, M.; Montiel, A. Retention of Copper and Nickel from Aqueous Solutions Using Manganese Oxide-Coated Burned Brick. *Environ. Prog. Sustain. Energy* **2012**, *31*, 426–434. [[CrossRef](#)]
25. Allahdin, O.; Dehou, S.C.; Wartel, M.; Recourt, P.; Trentesaux, M.; Mabingui, J.; Boughriet, A. Performance of FeOOH-brick based composite for Fe(II) removal from water in fixed bed column and mechanistic aspects. *Chem. Eng. Res. Des.* **2013**, *91*, 2732–2742. [[CrossRef](#)]
26. Xiaoran, Z.; Mingchen, Q.; Ziyang, Z.; Ranran, S.; Zheng, L.; Haiyan, L. Removal of Zn(II) from aqueous solutions by adsorption using different types of waste bricks. *Desalin. Water Treat.* **2018**, *106*, 177–190.
27. Allahdin, O.; Wartel, M.; Tricot, G.; Revel, B.; Boughriet, A. Hydroxylation and dealumination of a metakaolinite-rich brick under acid conditions, and their influences on metal adsorption: One- and two-dimensional (¹H, ²⁷Al, ²³Na, ²⁹Si) MAS NMR, and FTIR studies. *Microporous Mesoporous Mater.* **2016**, *226*, 360–368. [[CrossRef](#)]
28. Kołodzyńska, D.; Krukowska, J.; Thomas, P. Comparison of Sorption and Desorption Studies of Heavy Metal Ions From Biochar and Commercial Active Carbon. *Chem. Eng. J.* **2017**, *307*, 353–363. [[CrossRef](#)]
29. Priyantha, N.; Bandaranayaka, A. Investigation of kinetics of Cr(VI)-fired brick clay interaction. *J. Hazard. Mater.* **2011**, *188*, 193–197. [[CrossRef](#)]
30. Kumar, R.; Ansari, M.O.; Barakat, M.A. Adsorption of Brilliant Green by Surfactant Doped Polyaniline/MWCNTs Composite: Evaluation of the Kinetic, Thermodynamic, and Isotherm. *Ind. Eng. Chem. Res.* **2014**, *53*, 7167–7175. [[CrossRef](#)]
31. Boujelben, N.; Bouzid, J.; Elouear, Z. Studies of lead retention from aqueous solutions using iron-oxide-coated sorbents. *Environ. Technol.* **2009**, *30*, 737–746. [[CrossRef](#)] [[PubMed](#)]
32. Sun, K.; Shi, Y.; Wang, X.; Li, Z. Sorption and retention of diclofenac on zeolite in the presence of cationic surfactant. *J. Hazard. Mater.* **2017**, *323*, 584–592. [[CrossRef](#)] [[PubMed](#)]
33. Kubilay, Ş.; Gürkan, R.; Savran, A.; Şahan, T. Removal of Cu(II), Zn(II) and Co(II) ions from aqueous solutions by adsorption onto natural bentonite. *Adsorp.-J. Int. Adsorp. Soc.* **2007**, *13*, 41–51. [[CrossRef](#)]
34. Zanin, E.; Scapinello, J.; de Oliveira, M.; Rambo, C.L.; Franscescon, F.; Freitas, L.; de Mello, J.M.M.; Fiori, M.A.; Oliveira, J.V.; Dal Magro, J. Adsorption of heavy metals from wastewater graphic industry using clinoptilolite zeolite as adsorbent. *Process Saf. Environ. Prot.* **2017**, *105*, 194–200. [[CrossRef](#)]
35. Panday, K.K.; Prasad, G.; Singh, V.N. Copper(II) removal from aqueous solutions by fly ash. *Water Res.* **1985**, *19*, 869–873. [[CrossRef](#)]
36. Bhattacharyya, K.G.; Gupta, S.S. Adsorption of a few heavy metals on natural and modified kaolinite and montmorillonite: A review. *Adv. Colloid Interface Sci.* **2008**, *140*, 114–131. [[CrossRef](#)] [[PubMed](#)]
37. Abdel Salam, O.E.; Reiad, N.A.; ElShafei, M.M. A study of the removal characteristics of heavy metals from wastewater by low-cost adsorbents. *J. Adv. Res.* **2011**, *2*, 297–303. [[CrossRef](#)]
38. Babel, S.; Kurniawan, T.A. Low-cost adsorbents for heavy metals uptake from contaminated water: A review. *J. Hazard. Mater.* **2003**, *97*, 219–243. [[CrossRef](#)]
39. Crini, G. Recent developments in polysaccharide-based materials used as adsorbents in wastewater treatment. *Prog. Polym. Sci.* **2005**, *30*, 38–70. [[CrossRef](#)]
40. Djeribi, R.; Hamdaoui, O. Sorption of copper(II) from aqueous solutions by cedar sawdust and crushed brick. *Desalination* **2008**, *225*, 95–112. [[CrossRef](#)]
41. Abollino, O.; Aceto, M.; Malandrino, M.; Sarzanini, C.; Mentasti, E. Adsorption of heavy metals on Na-montmorillonite. Effect of pH and organic substances. *Water Res.* **2003**, *37*, 1619–1627. [[CrossRef](#)]
42. Aziz, H.A.; Adlan, M.N.; Ariffin, K.S. Heavy metals (Cd, Pb, Zn, Ni, Cu and Cr(III)) removal from water in Malaysia: Post treatment by high quality limestone. *Bioresour. Technol.* **2008**, *99*, 1578–1583. [[CrossRef](#)] [[PubMed](#)]

43. Afroze, S.; Sen, T.K.; Ang, H.M. Adsorption removal of zinc (II) from aqueous phase by raw and base modified Eucalyptus sheathiana bark: Kinetics, mechanism and equilibrium study. *Process Saf. Environ. Prot.* **2016**, *102*, 336–352. [[CrossRef](#)]
44. Lodeiro, P.; Herrero, R.; Sastre de Vicente, M.E. Batch desorption studies and multiple sorption–regeneration cycles in a fixed-bed column for Cd(II) elimination by protonated Sargassum muticum. *J. Hazard. Mater.* **2006**, *137*, 1649–1655. [[CrossRef](#)] [[PubMed](#)]
45. Aksu, Z.; Gönen, F. Biosorption of phenol by immobilized activated sludge in a continuous packed bed: Prediction of breakthrough curves. *Process Biochem.* **2004**, *39*, 599–613. [[CrossRef](#)]
46. Demey, H.; Lapo, B.; Ruiz, M.; Fortuny, A.; Marchand, M.; Sastre, A. Neodymium Recovery by Chitosan/Iron(III) Hydroxide [ChiFer(III)] Sorbent Material: Batch and Column Systems. *Polymers* **2018**, *10*, 204. [[CrossRef](#)]
47. Jain, M.; Garg, V.K.; Kadirvelu, K. Cadmium(II) sorption and desorption in a fixed bed column using sunflower waste carbon calcium–alginate beads. *Bioresour. Technol.* **2013**, *129*, 242–248. [[CrossRef](#)]
48. Yuan, X.; Huang, H.; Zeng, G.; Li, H.; Wang, J.; Zhou, C.; Zhu, H.; Pei, X.; Liu, Z.; Liu, Z. Total concentrations and chemical speciation of heavy metals in liquefaction residues of sewage sludge. *Bioresour. Technol.* **2011**, *102*, 4104–4110. [[CrossRef](#)]
49. Li, H.; Ji, H. Chemical speciation, vertical profile and human health risk assessment of heavy metals in soils from coal-mine brownfield, Beijing, China. *J. Geochem. Explor.* **2017**, *183*, 22–32. [[CrossRef](#)]



© 2019 by the authors. Licensee MDPI, Basel, Switzerland. This article is an open access article distributed under the terms and conditions of the Creative Commons Attribution (CC BY) license (<http://creativecommons.org/licenses/by/4.0/>).